Operationally accessible entanglement of one-dimensional spinless fermions

Hatem Barghathi, Emanuel Casiano-Diaz, and Adrian Del Maestro
Department of Physics, University of Vermont, Burlington, Vermont 05405, USA

(Received 29 May 2019; published 20 August 2019)

For indistinguishable itinerant particles subject to a superselection rule fixing their total number, a portion of the entanglement entropy under a spatial bipartition of the ground state is due to particle fluctuations between subsystems and thus is inaccessible as a resource for quantum information processing. We quantify the remaining operationally accessible entanglement in a model of interacting spinless fermions on a one-dimensional lattice via exact diagonalization and the density matrix renormalization group. We find that the accessible entanglement exactly vanishes at the first-order phase transition between a Tomonaga-Luttinger liquid and phase separated solid for attractive interactions and is maximal at the transition to the charge density wave for repulsive interactions. Throughout the phase diagram, we discuss the connection between the accessible entanglement entropy and the variance of the probability distribution describing intrasubregion particle-number fluctuations.

DOI: 10.1103/PhysRevA.100.022324

I. INTRODUCTION

The entanglement of a quantum mechanical system can be exploited as a resource, allowing spatially separated parties to perform protocols (e.g., dense coding [1], teleportation [2], and quantum cryptography [3]) not feasible in a classical setting. The quantification of the exact amount of entanglement encoded in a given state is thus an important task that can be accomplished by studying the von Neumann entropy of a subsystem [4,5]. The situation can become more complicated in a condensed matter setting [6], especially when considering an eigenstate of some physical Hamiltonian governing a system of indistinguishable and itinerant interacting particles, whose total number is fixed. Unlike an optical system of photons, conservation of total particle number N for atoms or electrons may restrict the set of possible local operations, often referred to as a superselection rule (SSR) [7], and can potentially limit the amount of entanglement that can be physically accessed [8–13]. This can be understood as originating from the fundamental inability to create coherent superposition states with different particle number in a subsystem. As a result, entanglement due to particle fluctuations alone cannot be utilized without access to a global phase reference [14]. In a pioneering work, Wiseman and Vaccaro [15] demonstrated that by averaging the von Neumann entanglement entropy of spatial modes over sectors corresponding to all possible numbers of particles in the subsystem defining those modes, they could place an upper bound on the amount of entanglement that could be transferred to a quantum register using local operations and classical communication. This quantity, known as the *accessible entanglement entropy*, has been previously studied for few-particle [15–20] or noninteracting [21,22] systems. However, the interplay between interactions and an SSR fixing the total particle number has yet to be fully explored. This is especially acute as many of the proposed or currently implemented quantum simulators [23], including those employing ultracold atoms [24], trapped ions [25], and electrons [26,27], are subject to fixed total N.

In this paper, we perform a systematic study of the accessible entanglement in an interacting model of spinless fermions, (the "t-V model"), on a one-dimensional lattice, which is known to exhibit a host of interesting behavior [28], including first- and second-order quantum phase transitions between both classically ordered and quantum disordered phases. We employ large-scale exact diagonalization (ED) to study the ground-state entanglement as a function of interaction strength for systems including up to 32 sites at different filling fractions. We compute both the originally defined von Neumann measure of accessible entanglement [15], as well as its recently introduced Rényi generalization [22]. In order to investigate the finite-size scaling of the accessible entanglement near the quantum phase transition to the localized charge density wave state, we perform density matrix renormalization group (DMRG) calculations using the ITENSOR library [29].

In the limits of infinitely strong repulsive and attractive interactions, we derive analytical results for the accessible entanglement and find that in the thermodynamic limit, the accessible entanglement is constant and equal to $\ln 2$ at half-filling. At the interaction strength corresponding to the first-order phase transition, the ground state is "flat" with all possible spatial occupations of the fermions contributing with equal weight. Here, the accessible entanglement is identically zero at all filling fractions. This result indicates that all of the entanglement between spatial subsystems at the transition is purely due to classical particle-number fluctuations between subregions and thus the entanglement entropy is equivalent to the Shannon entropy of the corresponding probability distribution [21]. This is a fermionic example of what was previously found in Bose-Einstein condensates and squeezed states of the Dicke model [30]. In the intervening quantum liquid, where the microscopic system is described at low energies by Tomonaga-Luttinger liquid (TLL) theory, the accessible entanglement is reduced from the spatial entanglement for a spatial subregion of length ℓ by a subleading double log: $\sim \ln(K \ln \ell)$ where K is the Luttinger parameter. We confirm this asymptotic scaling [21] for finite-sized systems by

exploiting the exact solution of the t-V model to obtain K and determine that this behavior is predicated on the rapid convergence of the subsystem particle-number probability distribution to a continuous Gaussian. The discreteness of the local number of particles introduces corrections that are exponentially small in the width of the distribution which is substantial within the quantum liquid. The accessible entanglement is maximal at the quantum phase transition between the TLL and charge density wave and appears to diverge in the thermodynamic limit signaling its potential use as a diagnostic measure more akin to a susceptibility than an order parameter.

The generalization of the operationally accessible entanglement to the Rényi entropies described by an integer index α is of considerable interest, as these are amenable to measurement without access to the complete density matrix [31,32]. Recent work identified the unique Rényi generalization of accessible entanglement [22] and we have measured it via exact diagonalization for the ground state of the t-V model. We find that the reduction of entanglement due to the superselection rule fixing the total number of particles is well described by the classical Rényi entropy of the subsystem particle-number distribution. This is not true in general, but approximately holds here due to a near proportionality between rescaled and bare number fluctuations. This proportionality is quantified and it is eventually violated for sufficiently large Rényi indices. In the TLL phase where particle fluctuations between subregions are expected to be Gaussian, we explore the validity of a recent prediction for symmetry-resolved entanglement [33] and find deviations that can be attributed to the amplification of finite-size and ultraviolet cutoff effects for large Rényi index $\alpha \sim 10$.

The main contributions of this work include the following: (1) confirmation that a system of fermions with fixed total particle number may act as a substantial entanglement resource for quantum information applications; (2) the identification of putative power-law scaling of the exponential of the accessible entanglement entropy near the continuous quantum phase transition from a Tomonaga-Luttinger liquid to an insulator; this transition thus identifies a critical coupling strength between fermions where the maximal amount of entanglement can be transferred to a quantum register; (3) by quantifying the role of the classical probability distribution governing the number of particles in a spatial subregion in placing a bound on the von Neumann and Rényi generalized accessible entanglement entropies, we open up experimental and computational avenues for the analysis of fermionic many-body phases as candidate resource states.

In the remainder of this paper, we provide a careful definition of the accessible entanglement entropy and discuss a few physical situations where its behavior is currently understood. We then move on to the definition of the model in question, the t-V model, and derive a number of exact results in some analytically tractable limits. The full phase diagram is then explored via ED and DMRG, where we answer the question of the exact amount of entanglement that can be extracted from a finite-size system of interacting lattice fermions. We identify the importance of the probability distribution controlling subsystem particle-number occupation and conclude with a brief discussion on the effects of the finite system sizes under investigation and the role of the filling fraction.

II. ACCESSIBLE ENTANGLEMENT

A. Rényi entanglement entropy

The amount of entanglement that exists between some partition A and its complement $\bar{A}$ of a quantum many-body system in pure state $|\Psi\rangle$ can be quantified via the Rényi entanglement entropy, which depends on an index α:

$$S_\alpha(\rho_A) = \frac{1}{1-\alpha} \ln \mathrm{Tr}\, \rho_A^\alpha, \tag{1}$$

where ρ_A is the reduced density matrix of partition A obtained by tracing out all degrees of freedom in $\bar{A}$ from the full density matrix:

$$\rho_A = \mathrm{Tr}_{\bar{A}}\, \rho = \mathrm{Tr}_{\bar{A}} |\Psi\rangle\langle\Psi|. \tag{2}$$

The Rényi entropy is a nonincreasing function of α and for $\alpha > 1$ is bounded from above by the von Neumann entropy $S_1(\rho_A) = -\mathrm{Tr}\rho_A \ln \rho_A$.

For a quantum many-body system subject to physical laws conserving some quantity (particle number, charge, spin, etc.), the set of local operations on the state $|\Psi\rangle$ is limited to those that do not violate the corresponding global superselection rule. For the remainder of this paper, we will focus on our discussion on the case of fixed total N and thus we are restricted to only those operators which locally preserve the particle number in A. The effect this has on the amount of entanglement that can be transferred to a qubit register is apparent from the simple example (adapted from Ref. [16]) of one particle confined to two spatial modes A and $\bar{A}$ corresponding to site occupations. Then, for the state $|\Psi\rangle = (|1\rangle_A \otimes |0\rangle_{\bar{A}} + |0\rangle_A \otimes |1\rangle_{\bar{A}})/\sqrt{2}$, Eq. (1) gives that $S_1 = \ln 2$. However, this entanglement cannot be transferred to a register prepared in initial state $|0\rangle_R$ via a SWAP gate:

$$\begin{aligned}&\mathrm{SWAP}|0\rangle_R \otimes (|1\rangle_A \otimes |0\rangle_{\bar{A}} + |0\rangle_A \otimes |1\rangle_{\bar{A}})/\sqrt{2} \\ &\quad = \frac{1}{\sqrt{2}}(|1\rangle_R \otimes |0\rangle_A \otimes |0\rangle_{\bar{A}} + |0\rangle_R \otimes |0\rangle_A \otimes |1\rangle_{\bar{A}}),\end{aligned}$$

where the first term is not physically allowable due to the restriction that the number of particles in the system is fixed to be one. The post-SWAP result remains in a product state and the amount of transferable entanglement is identically zero.

B. von Neumann accessible entanglement: $\alpha = 1$

Thus, Eq. (1), which includes the effects of nonlocal number fluctuations between A and $\bar{A}$, overcounts the amount of entanglement that can be accessed from the system. To quantify the physical reduction, Wiseman and Vaccaro [15] suggested that, for the case of $\alpha = 1$, a more appropriate measure should weight contributions to the entanglement coming from each superselection sector corresponding to the number of particles n in A:

$$S_1^{\mathrm{acc}}(\rho_A) = \sum_{n=0}^{N} P_n S_1(\rho_{A_n}). \tag{3}$$

Here, ρ_{A_n} is defined to be the reduced density matrix of A, projected onto the subspace of fixed local particle number n,

$$\rho_{A_n} = \frac{1}{P_n} \mathcal{P}_{A_n} \rho_A \mathcal{P}_{A_n}, \tag{4}$$

accomplished via a projection operator $\mathcal{P}_{A_n}$ that acts locally in partition A fixing the number of particles in it to n and the conservation of the total number of particles N guarantees $N-n$ particles in its complement $\bar{A}$. The probability of finding n particles in A is given by

$$P_n = \mathrm{Tr}\,\mathcal{P}_{A_n}\rho_A\mathcal{P}_{A_n} = \langle\Psi|\mathcal{P}_{A_n}|\Psi\rangle. \tag{5}$$

As the projection constitutes a local operation which can only decrease entanglement, it is clear that $S_1^{\mathrm{acc}}(\rho_A) \leqslant S_1(\rho_A)$. Moreover, the difference

$$\Delta S_1(\rho_A) \equiv S_1(\rho_A) - S_1^{\mathrm{acc}}(\rho_A) \tag{6}$$

can be determined by noting that the superselection rule guarantees that $[\rho_A, \hat{n}] = 0$ where $\hat{n}$ is the number operator acting in partition A. Thus, ρ_A is block diagonal in n and it can be shown [21] that

$$\Delta S_1(\rho_A) = H_1(\{P_n\}), \tag{7}$$

where

$$H_1(\{P_n\}) = -\sum_{n=0}^{N} P_n \ln P_n \leqslant \frac{1}{2}\ln\left(2\pi e\sigma^2 + \frac{1}{12}\right) \tag{8}$$

is the Shannon entropy of the number probability distribution where

$$\sigma^2 \equiv \langle n^2\rangle - \langle n^2\rangle = \sum_{n=0}^{N} n^2 P_n - \left(\sum_{n=0}^{N} nP_n\right)^2. \tag{9}$$

If P_n is a discrete Gaussian distribution, $P_n \propto \exp[-(n-\langle n\rangle^2)/(2\sigma^2)]$ with $\langle n\rangle \gg \sigma \gg 1$, then the von Neumann entanglement entropy is reduced by an amount which only depends on the variance $\Delta S_1 = \frac{1}{2}\ln(2\pi e\sigma^2)$.

C. Rényi accessible entanglement: $\alpha \neq 1$

Computing the accessible entanglement for a many-body system is a difficult task for $\alpha = 1$, as full state tomography is required to reconstruct the density matrix ρ. However, for integer values with $\alpha > 1$ a replica trick can be used to recast $\mathrm{Tr}\rho_A^\alpha$ as the expectation value of some local operator [31]. This advance has led to a boon of new entanglement results using both computational [19,34–37] and experimental [32,38–42] methods. Motivated by this progress, two of us recently generalized the accessible entanglement to the case of Rényi entropies with $\alpha \neq 1$ and found that [22]

$$S_\alpha^{\mathrm{acc}}(\rho_A) = \frac{\alpha}{1-\alpha}\ln\left[\sum_n P_n e^{\frac{1-\alpha}{\alpha}S_\alpha(\rho_{A_n})}\right] \tag{10}$$

which reproduces Eq. (3) in the limit $\alpha \to 1$. While not physically transparent in this form, the modification from the $\alpha = 1$ case results from replacing the geometric mean in Eq. (3) with a general power mean whose form is constrained by the physical requirement that

$$0 \leqslant \Delta S_\alpha \leqslant \ln(N+1), \tag{11}$$

where the upper bound is equal to the support of P_n. Equation (10) can also be interpreted as the quantum generalization of the conditional classical Rényi entropy [43–47], subject to physical constraints [22]. The arguments leading to Eq. (7) can then be generalized (see the Supplemental Material of Ref. [22]) leading to

$$\Delta S_\alpha \equiv S_\alpha - S_\alpha^{\mathrm{acc}} = H_{1/\alpha}(\{P_{n,\alpha}\}), \tag{12}$$

where we introduce the classical Rényi entropy of P_n

$$H_\alpha(\{P_n\}) = \frac{1}{1-\alpha}\ln\sum_n P_n^\alpha, \tag{13}$$

and

$$P_{n,\alpha} = \frac{\mathrm{Tr}\left[\mathcal{P}_{A_n}\rho_A^\alpha\mathcal{P}_{A_n}\right]}{\mathrm{Tr}\,\rho_A^\alpha} = \frac{P_n^\alpha \mathrm{Tr}\,\rho_{A_n}^\alpha}{\mathrm{Tr}\,\rho_A^\alpha} \tag{14}$$

can be interpreted as a normalization of partial traces of ρ_A^α, where the SSR fixing the total particle number leads to $\mathrm{Tr}\,\rho_A^\alpha = \sum_n \mathrm{Tr}\,[\mathcal{P}_{A_n}\rho_A^\alpha\mathcal{P}_{A_n}]$ and thus guarantees the normalization of $P_{n,\alpha}$. Note that we have defined $P_{n,1} \equiv P_n$ for notational consistency. For brevity, let $H_\alpha(\{P_n\}) \equiv H_\alpha$ from here onward.

Writing the difference ΔS_α as the classical Rényi entropy of the fictitious probability distribution $P_{n,\alpha}$, simplifies the calculation of ΔS_α and clarifies its properties, e.g., the fact that H_α is positive and bounded from above by $H_0 = \ln(N+1)$ guarantees that ΔS_α satisfies the physical requirement in Eq. (11) [22]. In addition, $P_{n,\alpha}$ is fully determined by P_n and the full and the projected traces of ρ_A^α, i.e., $\mathrm{Tr}\,\rho_A^\alpha$ and $\mathrm{Tr}\,\rho_{A_n}^\alpha$, which can be measured using the experimental and numerical methods mentioned above.

Before proceeding to a discussion of previous results for the accessible entanglement entropy, let us consider the special case where the probability distribution $P_{n,\alpha} \propto (P_n)^\alpha$. Then, using Eq. (12) we have

$$\begin{aligned}\Delta S_\alpha &= \frac{1}{1-\alpha^{-1}}\ln\sum_n\left(\frac{P_n^\alpha}{\sum_n P_n^\alpha}\right)^{1/\alpha} \\ &= H_\alpha,\end{aligned} \tag{15}$$

which reproduces the von Neumann result in Eq. (7).

D. Previous results

While the accessible entanglement entropy can be used to diagnose the feasibility of using a many-body state of quantum matter as an entanglement resource, exact results are mostly limited to noninteracting systems. For a condensate of free bosons, the projected reduced density matrix ρ_{A_n} is always pure for any n and thus the accessible entanglement is zero [19]. For free fermions, early calculations [18] found $S_1^{\mathrm{acc}} \neq 0$ in a thermal state under a noncontiguous spatial bipartition of two sites on a one-dimensional lattice. More recent work on noninteracting spinless fermions [21,22] found that the SSR fixing the total particle number reduces the accessible entanglement by an amount that is subleading in the size of the spatial bipartition ℓ when $\ell \gg 1$. This result hinges on the realization that the probability distribution $P_{n,\alpha}$ defined in Eq. (14) is Gaussian with an average that is independent of α and a variance σ_α^2 that scales as $\ell^{d-1}\ln\ell/\alpha$ in d spatial dimensions. This was recently confirmed on lattice in $d = 1$ [48]. As the spatial entanglement S_α scales as $\ell^{d-1}\ln\ell$ [49], $\Delta S_\alpha/S_\alpha \sim \ln(\ell^{d-1}\ln\ell)/(\ell^{d-1}\ln\ell)$ which vanishes as $\ell \to \infty$.

For critical systems in one dimension (1D) described by Luttinger liquid theory [or more generally any conformal field theory with a conserved U(1) current], the particle-number probability distribution P_n is also asymptotically Gaussian with a variance $\sigma^2 = K \ln \ell/\pi^2$ in the limit $\ell \gg 1$ [21,50–52], where K is the Luttinger parameter. Here, a result by Goldstein and Sela [33] can be employed to investigate $P_{n,\alpha}$, which is Gaussian, having the same average as P_n but with modified variance: $\sigma_\alpha^2 = \sigma^2/\alpha \overset{\ell\gg1}{\to} K/\alpha\pi^2 \ln \ell$. As a result,

$$\begin{aligned}\Delta S_\alpha|_{\rm TLL} &= H_{1/\alpha}(\{P_{n,\alpha}\}) = H_\alpha \\ &= \tfrac{1}{2}\ln\sigma^2 + \tfrac{1}{2}\ln[2\pi\alpha^{1/(\alpha-1)}]. \end{aligned} \tag{16}$$

Equation (16) can be combined with the known result for the spatial entanglement entropy of a critical 1D system [31,53,54]

$$S_\alpha|_{\rm 1D\,CFT} = \frac{c}{6}\left(1+\frac{1}{\alpha}\right)\ln\frac{\ell}{a_0} + O(1), \tag{17}$$

where c is the central charge and a_0 is a short-distance cutoff, to see that the fraction of nonaccessible entanglement entropy $\Delta S_\alpha/S_\alpha$ vanishes asymptotically as $\ln(\ln \ell)/\ln \ell$.

Studies of the interaction dependence of $S^{\rm acc}$ have been previously limited to bosonic systems in 1D. Quantum Monte Carlo simulations of harmonically trapped and harmonically interacting bosons identified maxima in the accessible entanglement as a function of interaction strength [19]. Exact diagonalization of the 1D Bose-Hubbard model at unit filling for systems of up to $N = 16$ demonstrated that $S_2^{\rm acc}$ vanishes in the limit of strong and weak interactions [20]. Interestingly, $S_2^{\rm acc}$ was maximal near the superfluid-insulator phase transition and appeared to obey phenomenological scaling for the limited system sizes that could be studied. For an extended Bose-Hubbard model of four modes that includes pair-correlated hopping, exact diagonalization and variational calculations identified an interesting regime with strong pair-correlations where a matter wave beam-splitter operation on the ground state results in all entanglement being accessible [55].

Missing from this list is any system of interacting fermions and we now present numerical results for spinless fermions in one spatial dimension.

III. THE t-V MODEL OF INTERACTING SPINLESS FERMIONS

A. Description and solution

To investigate the behavior of accessible entanglement in an interacting fermionic system, we consider the t-V model defined by a one-dimensional lattice of L sites occupied by N spinless fermions and governed by the Hamiltonian

$$H = -t\sum_i (c_i^\dagger c_{i+1} + c_{i+1}^\dagger c_i) + V\sum_i n_i n_{i+1}, \tag{18}$$

where $c_i^\dagger$ and c_i denote the fermionic creation and annihilation operators at site i, $\{c_i, c_j^\dagger\} = \delta_{i,j}$, and $n_i = c_i^\dagger c_i$. Here, $t > 0$ and V represent the nearest-neighbor hopping amplitude and interaction strength, respectively. We consider a half-filled lattice ($L = 2N$), unless mentioned otherwise and we use periodic boundary conditions (PBC) for an odd N, while for even N we use antiperiodic boundary conditions (APBC) to avoid complications arising from the degenerate ground state.

Equation (18) can be mapped onto the XXZ spin-$\frac{1}{2}$ chain (at fixed magnetization) which is exactly solvable via Bethe ansatz [28,56,57] (see, e.g., [58] for a recent pedagogical review). For $-2 < V/t < 2$, at low energies and long wavelengths, the system can be understood as a Tomonaga-Luttinger liquid where the TLL parameter K at half-filling is [59]

$$K = \frac{\pi}{2\cos^{-1}[-V/(2t)]}. \tag{19}$$

In this language, $0 < K < 1$ corresponds to repulsive ($V > 0$) interactions, $K > 1$ to attractive ($V < 0$) interactions, and noninteracting fermions ($V = 0$) have $K = 1$. By increasing the relative interaction strength $|V/t|$, the system undergoes two phase transitions, a first-order phase transition to a single fermionic cluster phase at $V/t = -2$, ($K = \infty$) and a continuous one at $V/t = 2$, ($K = 1/2$) to charge density wave (CDW) phase. A schematic phase diagram is shown in Fig. 1.

B. Exact ground-state results for accessible entanglement

In this section we derive a number of exact and asymptotic results for the accessible entanglement entropy of the t-V model using insights gained from the structure of the ground states depicted in Fig. 1. Results for the von Neumann accessible entanglement are summarized in Table I.

1. $V/t \to \infty$

In the limit $V/t \to \infty$ and at half-filling, the system reduces its energy by separating every two fermions by at least one empty site and thus the ground state $|\Psi_{V/t\to\infty}\rangle = (|\psi_{\rm even}\rangle + |\psi_{\rm odd}\rangle)/\sqrt{2}$ is an equal superposition of two occupation states. In one state the fermions occupy sites with only even indices ($|\psi_{\rm even}\rangle = |0101\ldots0101\rangle$) and in the other they occupy sites with only odd indices $|\psi_{\rm odd}\rangle = |1010\ldots1010\rangle$).

If we now consider spatial bipartition A consisting of ℓ consecutive sites, we can write

$$\begin{aligned}|\Psi_{V/t\to\infty}\rangle = &\frac{1}{\sqrt{2}}|\psi_{\rm even}\rangle_A \otimes |\psi_{\rm even}\rangle_{\bar A} \\ &+ \frac{1}{\sqrt{2}}|\psi_{\rm odd}\rangle_A \otimes |\psi_{\rm odd}\rangle_{\bar A}, \end{aligned} \tag{20}$$

resulting in the reduced density matrix

$$\rho_A = \tfrac{1}{2}|\psi_{\rm even}\rangle_A\langle\psi_{\rm even}| + \tfrac{1}{2}|\psi_{\rm odd}\rangle_A\langle\psi_{\rm odd}|.$$

For even ℓ, both of $|\psi_{\rm even}\rangle_A$ and $|\psi_{\rm odd}\rangle_A$ represent $\ell/2$ fermions as the number of sites with odd indices is equal to the number of sites with even indices. Therefore, the number of particles in partition A is fixed to $\ell/2$ and the entanglement entropy of the projected state $\mathcal{P}_{A_{n=\ell/2}}|\Psi_{V/t\to\infty}\rangle$ is $S_\alpha(\rho_{A_{n=\ell/2}}) = \ln 2$ with $P_{n=\ell/2} = 1$ resulting in an overall accessible entanglement entropy $S_\alpha^{\rm acc}(\rho_A) = \ln 2$. The picture is different for odd ℓ where the number of sites with odd indices differs from the number of sites with even indices by 1. In this case, one of the states $|\psi_{\rm even}\rangle_A$ and $|\psi_{\rm odd}\rangle_A$ will represent $(\ell-1)/2$ fermions while the other represents $(\ell+1)/2$ fermions and

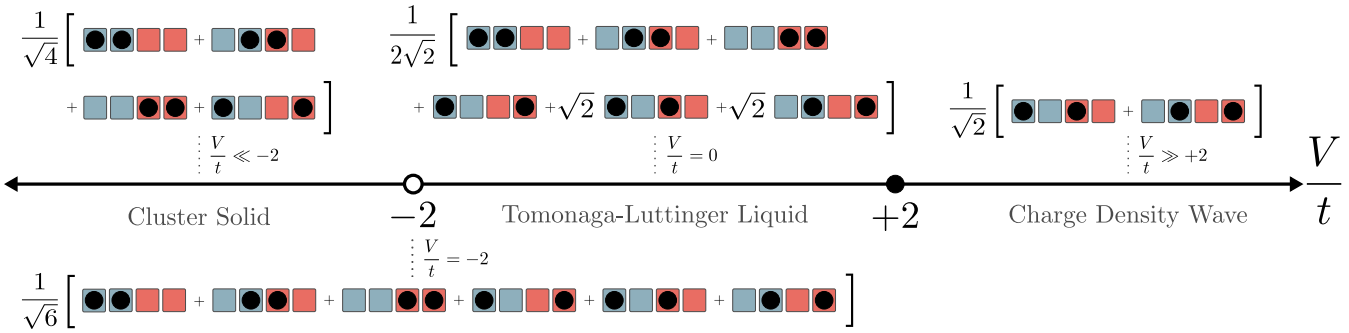

FIG. 1. Phase diagram of the t-V model accompanied by pictures of candidate ground states for $N = 2$ fermions on a $L = 4$ site lattice with antiperiodic boundary conditions. For the purposes of measuring accessible entanglement, the lattice has been bipartitioned into spatial subregions A (blue) and $\bar{A}$ (red), each of size $\ell = 2$. In the limit of strong attractive interactions where $V/t \ll -2$, the particles cluster together and there are L equally probable configurations corresponding to all translations of the cluster. At the first-order phase transition where $V/t = -2$, all $\binom{L}{N}$ configurations are equally probable resulting in a flat state. In the TLL phase with $|V/t| < 2$, particles are delocalized and we have included a characteristic state corresponding to free fermions ($V = 0$). In the limit of strong repulsive interactions where $V/t \gg 2$, fermions maximize their distance from each other resulting in a charge density wave (CDW) phase. The open and closed circles on the V/t axis denote a first-order and continuous phase transition, respectively.

therefore the projected state $\mathcal{P}_{A_{n=(\ell\pm1)/2}}|\Psi_{V/t\to\infty}\rangle$ is a separable state yielding zero entanglement entropy $S_\alpha^{\rm acc}(\rho_A) = 0$. For any partition size ℓ, regardless of its parity, the spectrum of ρ_A consists of two equal eigenvalues fixing the spatial entanglement entropy $S_\alpha(\rho_A)$ to $\ln 2$.

2. $V/t \to -\infty$

In the other extreme, $V/t \to -\infty$ and for any number of fermions $0 < N < L$, the system minimizes its energy by forming a cluster of fermions that extends over any consecutive N sites. The ground state of the system, in this case, is an equal superposition of all L possible clusters. Once more, considering a partition A of ℓ consecutive sites, we can write the ground state as

$$|\Psi_{V/t\to-\infty}\rangle = \frac{1}{\sqrt{L}}\sum_n\sum_{i,j}|n,i\rangle_A\otimes|N-n,j\rangle_{\bar{A}}, \qquad (21)$$

where $|n,i\rangle_A$ is the ith configuration having n particles in partition A and $|N-n,j\rangle_{\bar{A}}$ is the jth configuration with $N-n$ particles in its spatial complement $\bar{A}$. Since the state is a superposition of L particle configuration states, ρ_A can have at most L nonzero eigenvalues. This defines an upper bound on $S_\alpha(\rho_A) \leqslant \ln L$.

TABLE I. Analytical results for the accessible entanglement in the ground state of the t-V model with N fermions on L sites under a spatial bipartition consisting of $\ell = L/2$ contiguous sites. Symbols indicate approximations or generalizations with ♮ marking that the expression is asymptotically valid in the limit $L \gg 1$, † means $\ell < L$, and ‡ that the result is true for any filling fraction $N < L$.

Interaction	$S_1^{\rm acc}(\rho_A)$	ΔS_1
$V/t \to \infty$	$\frac{1}{2}[1+(-1)^\ell]\ln 2^{\dagger}$	$\frac{1}{2}[1-(-1)^\ell]\ln 2^{\dagger}$
$V/t \to -\infty$	$\frac{L-2}{L}\ln 2$	$\ln\frac{L}{2}^{\natural}$
$V/t = -2$	$0^{\dagger\ddagger}$	$\frac{1}{2}\ln L^{\natural}$

The simplicity of the state $|\Psi_{V/t\to-\infty}\rangle$ allows us to classify the projected state $\mathcal{P}_{A_n}|\Psi_{V/t\to-\infty}\rangle$ that corresponds to having n particles in partition A as follows. If the state $\mathcal{P}_{A_n}|\Psi_{V/t\to-\infty}\rangle$ has partition A or its complement $\bar{A}$ either empty or fully occupied, then $|\Psi_{V/t\to-\infty}\rangle$ must be a separable state with $S_\alpha(\rho_{A_n}) = 0$. What remains are the projected states $\mathcal{P}_{A_n}|\Psi_{V/t\to-\infty}\rangle$ in which both of A and $\bar{A}$ have at least one empty and one occupied site. Due to the existence of the fermion cluster, knowing the configuration of the n particles in partition A fully determines the configuration of the $N-n$ particles in partition $\bar{A}$. Moreover, there can be only two such configurations that correspond to the fermionic cluster emerging into the partition A, either from its left or right end, such that $\mathcal{P}_{A_n}|\Psi_{V/t\to-\infty}\rangle = \frac{1}{\sqrt{L}}\sum_{i=1}^{2}|n,i\rangle_A\otimes|N-n,i\rangle_{\bar{A}}$, where $\langle n,1|n,2\rangle_A = \langle N-n,1|N-n,2\rangle_{\bar{A}} = 0$. This gives $S_\alpha(\rho_{A_n}) = \ln 2$ and $P_n = 2/L$. A simple counting then gives the number of projected states m that yield nonzero entanglements as $\min\{\ell, L-\ell, N, L-N\} - 1$. The resulting accessible entanglement is given by

$$S_\alpha^{\rm acc}(\rho_A) = \frac{\alpha}{1-\alpha}\ln\left[\frac{2m}{L}2^{\frac{1-\alpha}{\alpha}} + 1 - \frac{2m}{L}\right], \qquad (22)$$

which simplifies to

$$S_1^{\rm acc}(\rho_A) = \frac{2m}{L}\ln 2, \qquad (23)$$

in the von Neumann case $\alpha = 1$. From Eq. (22) we see that $S_\alpha^{\rm acc}(\rho_A)$ is an increasing function of m. For a given L, the maximum value of m is $L/2-1$ which is achieved for $\ell = N = L/2$. In this case, $S_1^{\rm acc}(\rho_A) = \frac{L-2}{L}\ln 2$ and for $L \gg 1$ we can write $S_\alpha^{\rm acc}(\rho_A) \approx \ln 2$.

To calculate the spatial entanglement entropy of this state, in general, we need the full spectrum of ρ_A. Based on the above there will be $2m$ eigenvalues of ρ_A that are equal to $1/L$. In addition, there are two more eigenvalues which correspond to one of the partitions being either empty or fully occupied. Counting the number of such occupation states gives the eigenvalues $(|\ell - N| + 1)/L$ and $(|\ell + N - L| + 1)/L$. Now, if we consider the conditions for maximizing $S_\alpha^{\rm acc}(\rho_A)$, i.e., at

half-filling and with half-partition, we find that ρ_A has a flat spectrum with L eigenvalues and thus $S_\alpha(\rho_A)$ is saturated at its upper bound $S_\alpha(\rho_A) = \ln L$, and therefore $\Delta S_\alpha \approx \ln(L/2)$, for $L \gg 1$.

3. $V/t = -2$

Now, we turn our attention to the very interesting case of the first-order phase transition at $V/t = -2$, where the ground state $|\Psi_{V/t=-2}\rangle$ is an equal superposition of all $\binom{L}{N}$ possible configurations of N fermions on L sites (see Appendix for proof). In the language of the XXZ model, this corresponds to the isotropic ferromagnetic point [60]. If we project $|\Psi_{V/t=-2}\rangle$ into a state with n particles in partition A and in one of its $\binom{\ell}{n}$ possible configurations, we get an equal superposition of $\binom{L-\ell}{N-n}$ occupation states which differ only by the configuration of the $N-n$ particles in $\bar{A}$. Therefore, we can immediately construct the desired Schmidt decomposition by inspection:

$$|\Psi_{V/t=-2}\rangle = \frac{1}{\sqrt{\binom{L}{N}}} \sum_n \sqrt{\binom{\ell}{n}\binom{L-\ell}{N-n}} |n\rangle_A \otimes |N-n\rangle_{\bar{A}}. \tag{24}$$

Here, each of the normalized states $|n\rangle_A$ and $|N-n\rangle_{\bar{A}}$ is an equal superposition of all of the possible configurations of n and $N-n$ particles in partitions A and $\bar{A}$, respectively.

For the state above, the projected reduced density matrix $\rho_{A_n} = |n\rangle_A\langle n|_A$ is a pure state and, thus, for any n, $S_\alpha(\rho_{A_n}) = 0$. As a result, for any partition size ℓ, the accessible entanglement $S_\alpha^{\rm acc}(\rho_A) = 0$. Moreover, the spectrum of ρ_A is given by the particle-number probability distribution $P_n = \binom{\ell}{n}\binom{L-\ell}{N-n}/\binom{L}{N}$ where we have used the fact that the block-diagonal structure of ρ_A in n allows us to write $\rho_A = \sum_n P_n \rho_{A_n}$. Furthermore, for this state, $S_\alpha(\rho_A) = H_{1/\alpha}(\{P_{n,\alpha}\}) = H_\alpha(\{P_n\})$.

Let us consider the behavior of $S_\alpha(\rho_A)$ in the limit $L \gg 1$ and, for clarity, we focus on an equal bipartition at half-filling: $\ell = N = L/2$. Here, $P_n = \binom{\ell}{n}^2/\binom{2\ell}{\ell}$ and asymptotically it is a Gaussian distribution in n with variance $\sigma^2 = L/16$ and thus $S_\alpha(\rho_A) = \Delta S_\alpha = \frac{1}{2}\ln(2\pi\sigma^2\alpha^{(\alpha-1)^{-1}}) \approx \frac{1}{2}\ln L$.

IV. NUMERICAL RESULTS

To test the validity of the predictions in the previous section, we calculate the accessible entanglement in the ground state of the t-V model, defined in Sec. III, via numerical exact diagonalization for small systems (up to 32 sites) and using DMRG for larger systems (up to 98 sites), where the calculations are performed using the ITENSOR C++ library [29]. All data, code, and scripts used in this paper, including that needed to regenerate all figures, can be found online [61].

Before proceeding to an exposition of our numerical results, we summarize the main findings of this section: (1) at half-filling ($N = L/2$) and with a spatial partition size of $\ell = L/2$ contiguous sites, the numerically determined accessible entanglement confirms the asymptotic analytical predictions given in Table I and appears to be maximal at the phase transition between the quantum liquid and insulating CDW phases. (2) The reduction of entanglement due to the restriction of a fixed total number of particles can be understood in terms of the variance of the local particle-number distribution P_n, which is well characterized by a Gaussian distribution throughout the TLL phase. (3) This is approximately true even at Rényi index $\alpha > 1$ due to an emergent proportionality $P_{n,\alpha} \propto P_n^\alpha$ where $P_{n,\alpha}$ is the renormalized distribution defined in Eq. (14). (4) An analysis of subleading corrections in the partition size ℓ is needed to capture the interaction dependence of the variance of the particle-number distribution in the TLL phase. Finally, (5) the asymptotic effects of changing both the filling fraction and partition size can be captured by a universal scaling function.

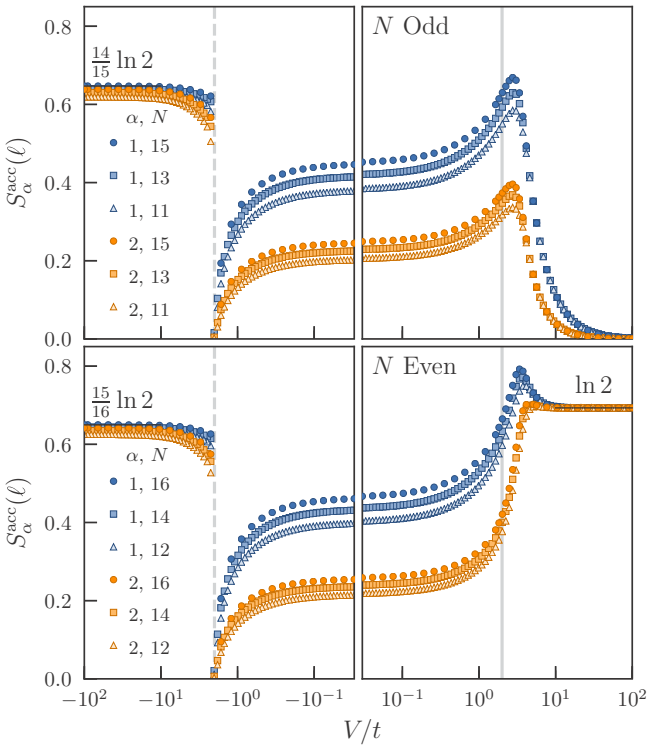

FIG. 2. Accessible entanglement entropy $S_\alpha^{\rm acc}(\ell)$ for $\alpha = 1, 2$ in the ground state of the t-V model as a function of interaction strength V/t at half-filling, $N = L/2$. The top panel shows the results for an odd number of total particles: $N = 11, 13, 15$ and the bottom, for even: $N = 12, 14, 16$. The solid and dashed gray vertical lines indicate the locations of the known phase transitions for the model $V/t = \pm 2$. For $N = 15, 16$ the asymptotic results computed in Sec. III in the limits $V/t \to \pm\infty$ for $S_1^{\rm acc}$ are shown as solid black lines.

A. Accessible entanglement

Figure 2 shows the von Neumann and second Rényi accessible entanglement entropies, $S_1^{\rm acc}$ and $S_2^{\rm acc}$, as a function of the dimensionless interaction strength $-100 \leqslant V/t \leqslant 100$ for the six largest systems studied by ED. To illustrate the effects that the parity of N has on $S_\alpha^{\rm acc}$, the top and bottom panels of Fig. 2 correspond to odd and even N, respectively. This represents the primary raw data set on which we base our analyses below.

B. Phase transitions and limiting cases of V/t

Starting from the regime of strong attractive interactions $V/t = -100$, in Fig. 2, we see that $S_1^{\rm acc}(\rho_A)$ is rapidly

converging to the expected value $(1-1/N)\ln 2$ in the limit $V/t \to -\infty$ [Eqs. (22) and (23)]. This asymptotic result persists down to nearly $V/t = -10$ for large system sizes. Increasing V/t further, $S_\alpha^{\rm acc}(\rho_A)$ decreases slowly until we get closer to the first-order phase transition at $V/t = -2$ (see Sec. III B 3), where $S_\alpha^{\rm acc}(\rho_A)$ decreases rapidly until it vanishes exactly at the transition point. This result holds for all N. As we increase V/t beyond -2, $S_\alpha^{\rm acc}(\rho_A)$ grows in the TLL regime, as interaction-driven liquid correlations build up, until it eventually peaks in the vicinity of the infinite system critical point ($V/t = 2$) and eventually saturate to its limiting $V/t \to \infty$ value by $V/t \simeq 100$ which depends on the particle-number parity: $S_\alpha^{\rm acc} \to 0$ for N odd and $S_\alpha^{\rm acc} \to \ln 2$ for N even. Exact diagonalization results up to $L = 32$ sites indicate that finite-size effects are most visible in the Tomonaga-Luttinger liquid phase and this is especially true as we approach the continuous phase transition at $V/t = 2$ where a maximum begins to develop in the accessible entanglement entropy.

Quantum information measures have been known for some time to show signatures at continuous and discrete phase transitions, both at $T = 0$ and finite temperature [62–75], including the case of spinless fermions under consideration here [64,76–79]. A commonality amongst these studies is that the information quantity in question (entanglement entropy, negativity, concurrence, purity, etc.) develops some feature akin to an order parameter. Here, an analysis of the exact diagonalization data shows that the accessible entanglement develops a maximum at a coupling strength $\frac{V}{t}|_{\rm max} \sim O(1)$. Making the empirical observation that the accessible entanglement appears to behave like a susceptibility, we perform an analysis of how the distance of the maximum from the infinite system size critical point ($\delta = \frac{V}{t}|_{\rm max} - 2$) depends on the system size L to search for power-law scaling.

In order to investigate the existence of such scaling using larger system sizes than are possible with ED, we employ DMRG where the total number of particles N is fixed and the resulting entanglement spectrum can be sorted according to the corresponding numbers of particles n and $N-n$ in the two partitions of the system [29]. This allows for the analysis of up to $L = 98$ sites at half-filling with the results shown in Fig. 3 where the DMRG is benchmarked against ED for $N = 15$ (periodic boundary conditions). Performing a two-parameter fit of the DMRG data to $\frac{V}{t}|_{\rm max} = 2 + \mathcal{A}N^{-1/\nu}$ supports a finite-size scaling form $\delta \sim L^{-1/\nu}$ ($L = 2N$), with exponent $1/\nu \simeq 0.3$.

C. Reduction of entanglement due to particle fluctuations between subsystems

The difference between the full and accessible von Neumann entanglement entropies $S_1 - S_1^{\rm acc} \equiv \Delta S_1 = H_1$ is equal to the Shannon entropy $H_1 = -\sum_n P_n \ln P_n$ of the particle-number distribution [21]. From the asymptotic results in Table I we expect ΔS_1 to be maximal in the limit of strong attractive interactions where it behaves like $\ln L$ as extensive particle fluctuations between spatial subsystems contribute to the entanglement. In the opposite limit $V/t \to \infty$, we expect the difference to converge to a constant (N odd) or zero (N even) where repulsion strongly suppresses number

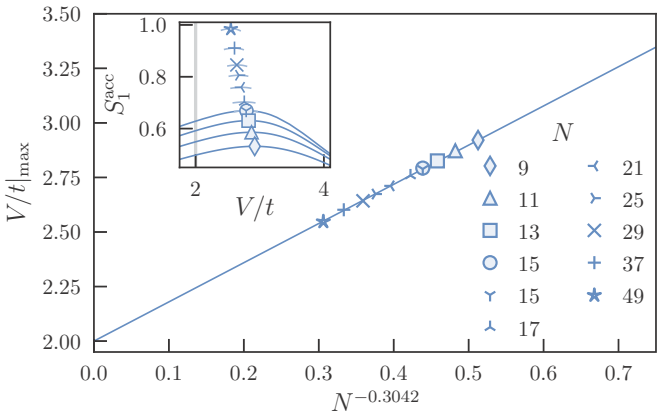

FIG. 3. Interaction strength at which the maximum $S_1^{\rm acc}$ occurs as a function of the total number of particles N. Filled shapes ($N \leqslant 15$) were computed with exact diagonalization while the remaining symbols for $N \geqslant 15$ are the result of density matrix renormalization group calculations. Finite-size corrections are investigated via a two-parameter fit of $\ln N$ vs $\ln(V/t - 2)$ and support scaling toward the infinite-size phase transition at $V/t = 2$. Inset: The interaction dependence of $S_1^{\rm acc}$ for various N in the neighborhood of $\frac{V}{t}|_{\rm max}$ shows an evolving peak.

fluctuations. This behavior is confirmed in Fig. 4 where we show the interaction dependence of ΔS_1 computed via exact diagonalization for $N = 15, 16$ (large circles). Figure 4 also includes the entanglement reduction computed from the numerically determined variance of P_n (small circles) under the assumption that P_n is a continuous Gaussian distribution with mean $\langle n\rangle$ described by

$$P_n \approx \frac{1}{\sqrt{2\pi\sigma^2}} \exp\left[\frac{-(n-\langle n\rangle)^2}{2\sigma^2}\right] \equiv \mathcal{N}(\langle n\rangle, \sigma^2) \qquad (25)$$

with associated Shannon entropy [see Eq. (16)]

$$H_1 = \Delta S_1 \approx \tfrac{1}{2}\ln(2\pi e\sigma^2).$$

The resulting agreement between the exact ΔS_1 with the asymptotic large-N result is surprisingly good over the entire range of $|V/t| \lesssim 2$ where P_n might still be expected to retain strong signatures of discreteness at these finite values of N. This is confirmed in the inset of the lower panel for $N = 16$ where we compare the exact finite-size probabilities P_n with a Gaussian distribution $\mathcal{N}(\langle n\rangle, \sigma^2)$ having the same mean $\langle n\rangle$ and variance σ^2 for a particular coupling $V/t = -1.5$.

Moreover, we can quantitatively capture the interaction dependence of ΔS_1 (solid lines in Fig. 4) using the predicted Gaussian form and variance of the number distribution at low energies within the TLL regime (in the thermodynamic limit) using $\sigma^2 = K\sigma_{\rm FF}^2$ [21,50,51] where the Luttinger parameter K is computed using Eq. (19) and $\sigma_{\rm FF}^2$ is the variance of P_n for free fermions. We note that we do not include a subleading interaction-dependent term in σ^2 to prevent overfitting.

To better understand the highly Gaussian nature of the subsystem particle-number probability distribution, we restrict to the case of even N, where the symmetry of P_n at half-filling guarantees that $\langle n\rangle = N/2$ is an integer such that $\delta n = n - \langle n\rangle$ is also an integer. Using the Poisson summation formula for a

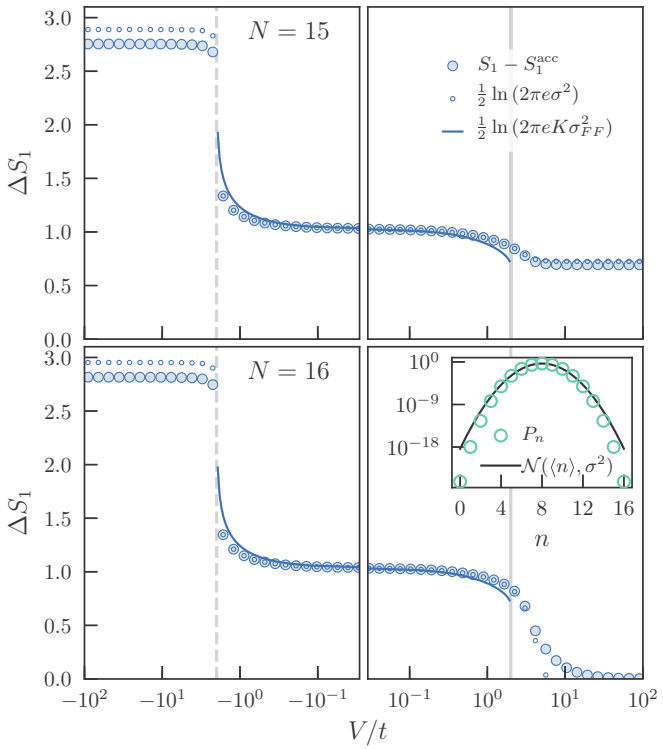

FIG. 4. Difference between the von Neumann and accessible entanglement entropies $\Delta S_1 = S_1 - S_1^{\rm acc}$ (large circles) and the Shannon entropy of a Gaussian distribution $\frac{1}{2}\ln 2\pi e\sigma^2$ (small circles) as functions of interaction strength V/t. Results were determined via exact diagonalization for the ground state of Eq. (18) with $N = 15, 16$. The observed agreement between the large and small symbols demonstrates the rapid convergence of P_n to a Gaussian distribution as seen in the inset for $V/t = -1.5$ where $\mathcal{N}(\langle n\rangle, \sigma^2)$ is a normal distribution with the same mean and variance as P_n. Solid lines are computed from the theoretical variance of the number of fermions in region A inside the Tomonaga-Luttinger liquid phase $\sigma^2 = K\sigma_{\rm FF}^2$, where K is the Luttinger parameter computed via Eq. (19) and $\sigma_{\rm FF}^2$ is the exact variance for free fermions ($V/t = 0$).

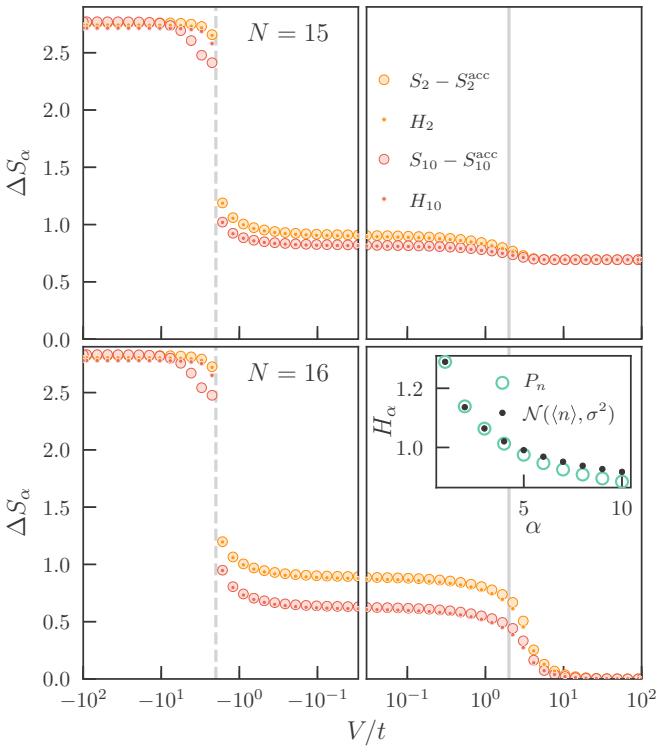

FIG. 5. Interaction dependence of the difference between the Rényi and accessible entanglement entropy $\Delta S_\alpha = S_\alpha - S_\alpha^{\rm acc}$. Large symbols are computed via exact diagonalization for the ground state of the t-V model at half-filling with a spatial partition corresponding to $L/2$ sites. Small symbols are the classical Rényi entropies H_α computed from P_n, the probability of finding n particles in the spatial subregion. We observe $H_\alpha \leqslant \Delta S_\alpha$ with the lower bound being nearly saturated over a wide range of interactions, but is worse for even N and as α is increased from 2 to 10. This is quantified in the inset which compares H_α computed from the exact probability distribution P_n at $V/t = -1.5$ with that obtained from a Gaussian with the same mean and variance as P_n for $N = 16$.

Gaussian function we find

$$\sum_{\delta n=-\infty}^{\infty} e^{-\frac{(\delta n)^2}{2\sigma^2}} = \sqrt{2\pi\sigma^2}\left[1 + 2\sum_{\delta n=1}^{\infty} e^{-2\pi^2\sigma^2(\delta n)^2}\right], \qquad (26)$$

where the summation on the right-hand side represents the error in the normalization of P_n which decreases with increasing variance σ^2 (the odd N case is analogous[1]). For the data presented in the inset of Fig. 4, the value of σ^2 is 0.772 ($N = 16$) leading to a corresponding error of $\sim 10^{-6}$. Taking the derivative of both sides of Eq. (26) with respect to σ^2 shows that the variance of P_n calculated using its expression in Eq. (25) is well approximated by σ^2 in the same limits.

We can extend this analysis to the case of Rényi indices $\alpha > 1$ with exact digonalization results shown in Fig. 5. Here, the difference between the spatial and accessible entanglement is no longer exactly equal to H_α, the classical Rényi entropy of P_n, but is instead given by the modified expression $H_{1/\alpha}(\{P_{n,\alpha}\})$ as defined in Eqs. (12)–(14). However, a comparison of the large and small symbols in Fig. 5 indicates that $\Delta S_\alpha \approx H_\alpha$ for $|V/t| \lesssim 2$. This can be understood using our observation from Fig. 4 that P_n is well approximated by a continuous Gaussian distribution in the TLL phase. In this case, the renormalized probability distribution $P_{n,\alpha} \approx (P_n)^\alpha / \sum_n (P_n)^\alpha$ is also Gaussian with variance $\sigma_\alpha^2 = \sigma^2/\alpha$. As shown in Eq. (15), this has the consequence that $H_{1/\alpha}(\{P_{n,\alpha}\}) \simeq H_\alpha$ and thus the difference $\Delta S_\alpha \simeq H_\alpha$. For larger values of α, increased deviations between ΔS_α and H_α are observed which are quantified in the inset of of the lower panel of Fig. 5 that compares H_α computed for the exact P_n at $V/t = -1.5$ with that determined from a continuous normal distribution having the same mean and variance as P_n for $N = 16$. For $\alpha = 10$, the effects of discreteness are amplified which can be understood by returning to Eq. (26) with $\sigma_\alpha^2 = \sigma^2/\alpha$ such that the correction term on the right-hand side becomes more important as the width of the distribution is squeezed.

[1]For odd N, the relevant Poisson summation formula is $\sum_{\delta n=-\infty}^{\infty} \exp[-(\delta n + 1/2)^2/(2\sigma^2)] = \sqrt{2\pi\sigma^2}\{1 + 2\sum_{\delta n=1}^{\infty}(-1)^{\delta n} \exp[-2\pi^2\sigma^2(\delta n)^2]\}$.

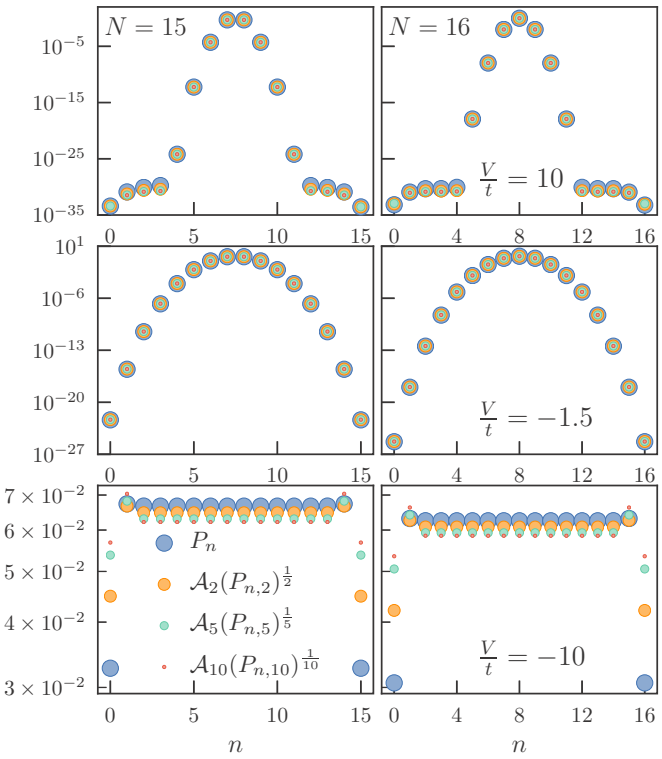

FIG. 6. Rescaling the effective probability distribution defined in Eq. (14) for the ground state of the t-V model at half-filling demonstrates the approximate proportionality relation $P_n \sim (P_{n,\alpha})^{1/\alpha}$ for interaction strengths corresponding to the charge density wave (top row, $V/t = 10$), Tomonaga-Luttinger liquid (middle row, $V/t = -1.5$), and cluster phases (bottom row, $V/t = -10$) for Rényi indices $\alpha = 1, 2, 5, 10$. $\mathcal{A}_\alpha^{-1} = \sum_n (P_{n,\alpha})^{1/\alpha}$ is a normalization constant and $P_{n,\alpha}$ is defined in Eq. (14). The shape of the distributions and their connection to the physical ground states of the t-V model are discussed in the text.

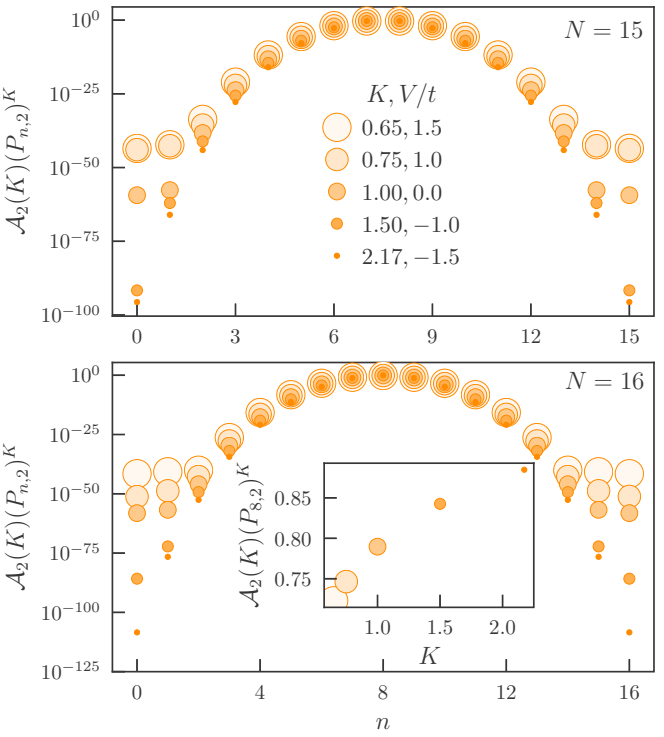

FIG. 7. The effective probability distribution $P_{n,\alpha=2}$ for the ground state of the t-V model at half-filling and for different interaction strengths V/t in the TLL phase is rescaled as $[P_{n,2}]^K$, were K is the corresponding Luttinger parameter computed from Eq. (19). While the probabilities seem to show collapse near the middle of the distribution where $n \simeq N/2$, the inset shows strong additional K dependence of the probability for fixed particle number $n = 8$ in A. As discussed in the text, this lack of collapse is due to the subleading interaction-dependent corrections to the asymptotic scaling of the variance σ^2 in Eq. (27).

D. Local particle-number distribution

The preceding analysis of the accessible entanglement entropy has demonstrated the importance of the specific form of the probability distribution P_n and in Fig. 6 we examine it more closely in the three phases of the t-V model. For large repulsive interactions where the system is in the CDW phase (top panel, $V/t = 10$), P_n is dominated by configurations where $n = N/2$ for N even and $n = (N \pm 1)/2$ for N odd. In the TLL phase where $|V/t| < 2$, we have already found that P_n is well described by a normal distribution (middle row, $V/t = -1.5$). Finally, for strong attractive interactions (bottom row, $V/t = -10$), P_n is nearly flat, as the ground state is a superposition of all spatial translations of the cluster of N particles. Figure 6 also explains the empirical observation of the semiequality $\Delta S_\alpha \approx H_\alpha$ for all interaction strengths as a consequence of the proportionality $P_{n,\alpha} \sim P_n^\alpha$ by demonstrating the collapse of $\mathcal{A}_\alpha P_{n,\alpha}^{1/\alpha}$ to P_n for different values of α, where $\mathcal{A}_\alpha$ is a normalization factor.

Motivated by the observation of the α collapse of the effective probability distribution $P_{n,\alpha}$, we test another asymptotic result: in the TLL phase the variance σ_α^2 is expected to approach the value of $K\sigma_{\mathrm{FF}}^2/\alpha$. This means that for a fixed α, we expect the asymptotically Gaussian distribution $P_{n,\alpha}(K)$ for a given interaction strength K to be proportional to $[P_{n,\alpha}(K = 1)]^{1/K}$. This prediction is investigated in Fig. 7, where we set $\alpha = 2$ and consider different interaction strengths in the TLL phase where we have used Eq. (19) to convert between V/t and the Luttinger parameter K. On a semilogarithmic scale, the results suggest data collapse to $P_{n,2}(K = 1)$ near the middle of the distributions corresponding to $n \simeq N/2$ particles in the subregion. However, a linear-linear analysis at $n = N/2$ exposes deviations, as illustrated in the inset of Fig. 7 (bottom panel). This can be understood by considering higher-order corrections to the asymptotic dependence of σ^2 on K, e.g., for $\alpha = 1$, the variance of P_n is given by [50]

$$\sigma^2 \simeq \frac{K}{\pi^2} \ln \ell + a_1 - \frac{a_2(-1)^\ell}{\ell^{2K}}, \tag{27}$$

where a_1 and a_2 are K-dependent constants and ℓ is the macroscopic size of the spatial subregion. We have tested that a more faithful rescaling of the distributions with $\sigma^2/\sigma_{\mathrm{FF}}^2$ instead of K leads to improved data collapse, especially if σ^2 and σ_{FF}^2 are calculated by fitting the middle portion of the distribution to a Gaussian function, instead of requiring them to be the variance of the corresponding distribution.

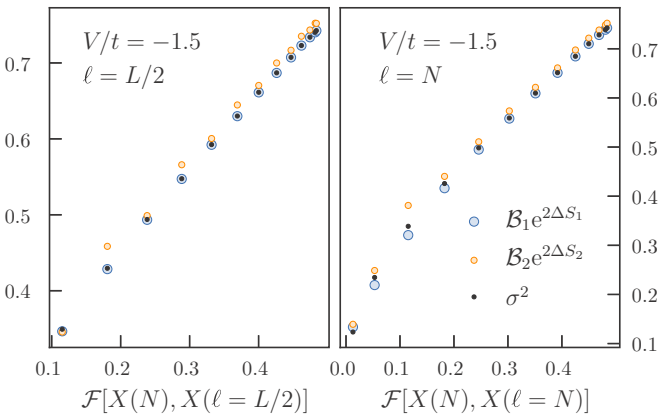

FIG. 8. The filling fraction dependence of the variance σ^2 (black dots) of the particle-number distribution P_n compared to that computed from the difference between the (exponentiated) accessible and spatial entanglement entropies for $\alpha = 1$ (large circles) and $\alpha = 2$ (small circles) using Eq. (29). Exact diagonalization results in the ground state of the t-V model with $V/t = -1.5$ and $L = 28$ demonstrate consistency with the predicted asymptotic scaling function $\mathcal{F}(N, \ell)$ given in Eq. (27) where we have fixed $\ell = L/2$ (left panel) or set $\ell = N$ (right panel) and changed N from $2 \ldots 14$. In order to reduce finite-size effects, both of the partition size ℓ and the total number of particles N are replaced by their corresponding chord length $X(\ell) = (L/\pi)\sin(\pi\ell/L)$ and $X(N)$, respectively. The constants $\mathcal{B}_1 = (\pi e)^{-1}$ and $\mathcal{B}_2 = (2\pi)^{-1}$ are used to rescale the entanglement reduction to obtain a prediction for the variance σ^2.

E. Results away from half-filling

Until now, we have focused on the case of a half-filled lattice: $N = L/2$. A more general result for the scaling of the variance of the particle-number distribution σ^2 (fluctuation entanglement) in the TLL phase for a system of size $L, N \gg 1$ but with a finite filling fraction N/L is given by [51,80]

$$\sigma^2 \approx \mathcal{F}(N, \ell) = \frac{K}{2\pi^2} \ln\left[\left(\frac{\pi N \ell}{L}\right)^2 + 1\right]. \tag{28}$$

In order to compute K above we note that when $N/L \neq \frac{1}{2}$, Eq. (19) is no longer valid and the V/t dependence of the Luttinger parameter must be determined via a full numerical solution of the Bethe ansatz equations for the corresponding XXZ model at each filling fraction N/L. For $\ell \gg 1$, the above expression simplifies to the known asymptotic result $\sigma^2 \approx (K/\pi^2)\ln(k_F \ell a_0)$[21], where $k_F = \pi N/(L a_0)$ is the Fermi momentum and a_0 is a microscopic length scale.

In Fig. 8, we explore the scaling prediction of Eq. (28). In the left panel we increase the number of fermions N in a system with a fixed system size $L = 28$ and partition size $\ell = L/2 = 14$, while in the right panel we set $L = 28$ but grow N and ℓ together, i.e., $\ell = N$. To take into account the finite-size and periodic boundary conditions in our exact diagonalization calculations we replace ℓ with the chord length $X(\ell) = (L/\pi)\sin(\pi\ell/L)$ and similarly N with $X(N)$. We observe that the numerical results are consistent with with Eq. (28) for a modest system size.

We also investigate the prediction that P_n should remain a Gaussian distribution, even away from half-filling by solving for σ^2 using Eq. (16) we find

$$\sigma^2 = \mathcal{B}_\alpha \exp(2\Delta S_\alpha), \tag{29}$$

where $\mathcal{B}_\alpha \equiv \alpha^{(1-\alpha)^{-1}}/\pi$ and taking the appropriate limit yields $\mathcal{B}_1 = (\pi e)^{-1}$. For $\alpha = 1$, we expect that Eq. (29) should asymptotically hold, as long as P_n is a Gaussian distribution with variance σ^2. This is confirmed by the agreement between the large circles and filled black dots in Fig. 8.

For $\alpha \neq 1$, the validity of Eq. (29) requires that both $P_{n,\alpha}$ is Gaussian, and that its variance σ_α^2 behaves as $\sigma_\alpha^2 = \sigma^2/\alpha$. In Fig. 8 we see that this is almost the case for $\alpha = 2$, where the small deviations can be attributed to the squeezed variance of $\sigma_2^2 = \sigma^2/2$ compared to σ^2 as discussed above. In other words, even if the most relevant part of P_n takes the form of a discrete Gaussian distribution, the value of the parameter σ^2 in the exponent of $\exp[-(\delta n)^2/(2\sigma^2)]$ can only approximately represent the variance of the true distribution, with an accuracy that increases with σ^2 as derived from Eq. (26). The weak oscillations which appear in Fig. 8 for $\alpha = 2$ are due to the same anomalous scaling corrections that appear in the Rényi entanglement entropy with $\alpha > 1$ [81].

V. DISCUSSION

In this paper we have presented a systematic study of how nearest-neighbor interactions affect the amount of operationally accessible entanglement that could be extracted from the ground state of a system of one-dimensional spinless lattice fermions where the total number of particles is fixed. The existence of this superselection rule (fixed N) limits the set of physical operations that can be performed with the result that the entanglement entropy under a spatial mode bipartition provides an absolute upper bound on the accessible entanglement. We have derived analytic results for the von Neumann ($\alpha = 1$) and generalized Rényi ($\alpha \neq 1$) accessible entanglement in a few special cases (see Table I). In the limit of strong attractive interactions, the ground state is a superposition of all translations of a single cluster of N fermions and the accessible entanglement is reduced by $\ln N$ from the spatial entanglement saturating at a constant for large N. For strong repulsive interactions at half-filling, the ground state is a superposition of possible density waves commensurate with the number of sites and the accessible entanglement is equal to the spatial entanglement for even N (no reduction), while it is reduced by a constant term to zero for odd N. Finally, exactly at the first-order phase transition at $V/t = -2$, the ground state is an equal weight superposition of all possible fermion occupation states and the accessible entanglement is identically zero for all filling fractions and system sizes. This constitutes the maximal possible reduction, with all of the spatial entanglement entropy, which scales as the logarithm of the subsystem size, being due to particle fluctuations. This result highlights the importance of understanding the role of classical number fluctuations in itinerant many-body systems when using entanglement entropy as a phase diagnostic. The drastic reduction in entanglement after projection into fixed particle-number subsectors is reminiscent of Yang's η-paired state [82] under the quantum disentangled liquid diagnostic [83–85] which involves a partial projection onto spin degrees of freedom.

Within the Tomonaga-Luttinger liquid phase $|V/t| < 2$ the asymptotic form of the particle-number distribution P_n is known to be Gaussian with a variance that scales as $\sigma^2 \simeq (K/\pi^2)\ln \ell$ for $\ell \gg 1$ [21,50]. σ^2 is parametrically large enough within the quantum liquid (especially for attractive interactions) that the discreteness of the underlying P_n distribution can be neglected. Fluctuations in this regime are not the only factor controlling entanglement, and the presence of interactions ensures that the spatial entanglement entropy is reduced by the superselection rule only by a subleading double logarithm. Thus, the fermionic Luttinger liquid at half-filling can be considered a useful entanglement resource.

At the continuous quantum phase transition between the TLL and charge density wave, we observe a global maxima in the accessible entanglement which demonstrates a susceptibilitylike scaling consistent with the known thermodynamic limit critical value of $V/t = 2$. Confirmation of this scaling, especially away from half-filling, would require studying larger system sizes than considered here. Ultimately, we are limited by the well-known difficulties of DMRG when investigating ground states with a large amount of entanglement [here scaling like $\sim \ln(L/2)$ for $\ell = L/2$] near the critical point, especially with periodic boundary conditions as considered here. There are many natural extensions of this work utilizing DMRG with access to quantum numbers describing subregion particle occupation numbers, including investigating the effects of boundary conditions, different partition sizes, and extended range interactions.

The difference between the von Neuman ($\alpha = 1$) accessible and spatial entanglement entropies, ΔS_1, is exactly given by the Shannon entropy H_1 of the corresponding particle-number distribution P_n [21]. A direct Rényi generalization of this relation to $\alpha \neq 1$ is not true [22], i.e., $\Delta S_\alpha \neq H_\alpha$. However, a sufficient condition for such a generalization is that $P_{n,\alpha} \propto (P_n)^\alpha$ where the constant of proportionality can be dependent on α but not on n. This is equivalent to requiring that the trace of the projected reduced density matrix raised to the power α, $\mathrm{Tr}\,\rho_{A_n}^\alpha$, be independent of n. This is always the case asymptotically for $\ell \gg 1$ when the number fluctuations are Gaussian with a variance σ_α^2 that is inversely proportional to α, ($|V/t| < 2$), but we find it to be approximately satisfied throughout the phase diagram, even away from half-filling. However, deviations occur in the limit of strong attractive interactions, or when $\alpha \gg 1$. In this case, large α always tends to reduce the variance of the effective distribution $P_{n,\alpha}$ and thus for finite-size systems, the discreteness of the physical number of particles in spatial subregion A can further spoil the semiequality between ΔS_α and H_α. The fact that $\Delta S_\alpha \approx H_\alpha$ when $V/t \gg 1$ is a consequence of the separation of scales in this limit where P_n is dominated by configurations with $n \simeq N/2$.

This result accentuates the importance of the superselection rule in reducing accessible entanglement and provides a direct route toward the experimental measurement of ΔS_α in systems of ultracold atoms via a quantum gas microscope [86]. The required experimental protocol is discussed in detail in Ref. [20] and an effective measurement of the fluctuation entanglement for a single site has already been reported in a quantum simulator of the Bose-Hubbard model [39]. Moving to fermions is more challenging, although similar replica-based methods have been previously employed [41].

Many open questions remain, and having demonstrated the utility of the operationally accessible entanglement in an exactly solvable model, it is natural to ask what this quantity can tell us about nonintegrable models in one dimension as well interacting fermions and soft-core bosons in higher dimensions. In the latter case, the support of P_n is no longer bounded by the number of sites in the spatial subregion, and the study of large systems could be performed via quantum Monte Carlo simulations [19]. Recent work validating the connection between subregion particle fluctuations and spatial entanglement in a nonequilibrium setting [87] could also be extended to probe how superselection rules may affect the dynamics of accessible entanglement after a quantum quench.

From a quantum information perspective, it seems important to further explore how the accessible entanglement relates to the plethora of measures [88–92] which do not directly include physical restrictions on N, but aim to quantify the technologically useful quantum correlations encoded in interacting and indistinguishable itinerant quantum particles.

ACKNOWLEDGMENTS

We benefited from discussion with C. M. Herdman, F. Heidrich-Meisner, I. Klich, and M. Stoudenmire. This research was supported in part by the National Science Foundation (NSF) under Award No. DMR-1553991 (A.D.). All computations were performed on the Vermont Advanced Computing Core supported in part by NSF Award No. OAC-1827314.

APPENDIX: GROUND STATE OF THE t-V MODEL FOR $V/t = -2$

Consider the Hamiltonian of the t-V model given in Eq. (18) at the special interaction strength $V = -2t$ corresponding to the first-order phase transition:

$$H = -t\sum_{i=1}^{L}(c_i^\dagger c_{i+1} + c_{i+1}^\dagger c_i) - 2t\sum_{i=1}^{L} n_i n_{i+1}, \tag{A1}$$

where we assume periodic boundary conditions for N even and antiperiodic boundary conditions for N odd.

1. Fermion occupation basis

We study the effect of H in the N fermion occupation basis $\{|\psi_a\rangle\}$, where the index a runs over all of the $\binom{L}{N}$ possible configurations. For example, for $N = 2$ and $L = 4$ there are six such states: $|\psi_a\rangle \in \{|1100\rangle, |1010\rangle, |1001\rangle, |0110\rangle, |0101\rangle, |0011\rangle\}$.

Starting with the potential operator $\mathcal{V} \equiv -2t\sum_{i=1}^{L} n_i n_{i+1}$ which is diagonal in this basis, we have

$$\mathcal{V}|\psi_a\rangle = -2t\, n_a^{(11)}|\psi_a\rangle, \tag{A2}$$

where $n_a^{(11)}$ counts the number of bonds connecting two occupied sites in the state $|\psi_a\rangle$. The hopping operator $\mathcal{T} \equiv -t\sum_{i=1}^{L}(c_i^\dagger c_{i+1} + c_{i+1}^\dagger c_i)$ turns $|\psi_a\rangle$ into a superposition of all the states $|\psi_b\rangle$ connected to $|\psi_a\rangle$ by moving one particle to

a neighboring empty site. We can write

$$\mathcal{T}|\psi_a\rangle = -t \sum_{b\in \mathsf{S}_a} |\psi_b\rangle, \tag{A3}$$

where S_a is the resulting index set of occupation states $|\psi_b\rangle$, i.e., $b \in \mathsf{S}_a \iff \langle\psi_b|\mathcal{T}|\psi_a\rangle \neq 0$. The cardinality of S_a is

$$\begin{aligned}\mathrm{card}(\mathsf{S}_a) &\equiv \sum_{b\in \mathsf{S}_a} 1 \\ &= n_a^{(10)} + n_a^{(01)} \\ &= 2N - 2n_a^{(11)},\end{aligned} \tag{A4}$$

where $n_a^{(10)}$ ($n_a^{(01)}$) counts the number of occupied-empty (empty-occupied) bonds in $|\psi_a\rangle$ and in the last line we have used the fact that the total number of particles on a ring is (independent of the index a)

$$N = n_a^{(11)} + \left(n_a^{(10)} + n_a^{(01)}\right)/2. \tag{A5}$$

A general matrix element in the fermion occupation basis is given by

$$\langle\psi_c|\mathcal{T}|\psi_a\rangle = -t \begin{cases} 1, & c \in \mathsf{S}_a \\ 0, & \text{otherwise} \end{cases} \tag{A6}$$

which is guaranteed to be real, thus,

$$\langle\psi_c|\mathcal{T}|\psi_a\rangle = \langle\psi_a|\mathcal{T}|\psi_c\rangle \Rightarrow c \in \mathsf{S}_a \iff a \in \mathsf{S}_c. \tag{A7}$$

This is a useful result that can be used to swap the order of restricted and unrestricted summations.

Let us now consider the action of $\mathcal{T}$ on a general state $|\Psi\rangle = \sum_a \mathcal{C}_a|\psi_a\rangle$ where $\mathcal{C}_a \in \mathbb{C}$:

$$\begin{aligned}\mathcal{T}|\Psi\rangle &= -t \sum_a \mathcal{C}_a \sum_{b\in \mathsf{S}_a} |\psi_b\rangle \\ &= -t \sum_c |\psi_c\rangle \sum_a \mathcal{C}_a \sum_{b\in \mathsf{S}_a} \langle\psi_c|\psi_b\rangle \\ &= -t \sum_c |\psi_c\rangle \left[\sum_a \mathcal{C}_a \sum_{b\in \mathsf{S}_a} \delta_{c,b}\right],\end{aligned} \tag{A8}$$

where we have inserted a resolution of the identity operator $\sum_c |\psi_c\rangle\langle\psi_c| = \mathbb{1}$ into the second line. Now, $\sum_{b\in \mathsf{S}_a} \delta_{c,b} \neq 0 \iff c \in \mathsf{S}_a$ and using Eq. (A7) we can write

$$\sum_a \mathcal{C}_a \sum_{b\in \mathsf{S}_a} \delta_{c,b} = \sum_{a\in S_c} \mathcal{C}_a. \tag{A9}$$

Substituting into Eq. (A8) above and relabeling $a \leftrightarrow c$ leads to the general result

$$\mathcal{T}|\Psi\rangle = -t \sum_a \sum_{c\in \mathsf{S}_a} \mathcal{C}_c|\psi_a\rangle. \tag{A10}$$

Written in this form, we can combine Eq. (A10) with Eqs. (A2) and (A4) to compute the action of the full Hamiltonian at $V = -2t$ on $|\Psi\rangle$:

$$\begin{aligned}H|\Psi\rangle &= -t \sum_a \left[\sum_{c\in \mathsf{S}_a} \mathcal{C}_c + 2n_a^{(11)}\mathcal{C}_a\right]|\psi_a\rangle \\ &= -2tN|\Psi\rangle - t \sum_a \sum_{c\in \mathsf{S}_a} (\mathcal{C}_c - \mathcal{C}_a)|\psi_a\rangle.\end{aligned} \tag{A11}$$

2. Flat state

From Eq. (A11) it is immediately apparent that the flat state

$$|\Psi_0\rangle = \frac{1}{\sqrt{\binom{L}{N}}} \sum_a |\psi_a\rangle \tag{A12}$$

is an eigenstate of H with energy $-2tN$. To prove that $|\Psi_0\rangle$ is indeed the ground state, we consider matrix elements of the shifted operator $H' = H + 2tN$ for a general state $|\Psi\rangle$ expanded in the fermion occupation basis:

$$\begin{aligned}\langle\Psi|H'|\Psi\rangle &= -t \sum_{a,b} \sum_{c\in \mathsf{S}_a} (\mathcal{C}_c - \mathcal{C}_a)\langle\psi_b|\psi_a\rangle\mathcal{C}_b^* \\ &= t \sum_a \sum_{c\in \mathsf{S}_a} (|\mathcal{C}_a|^2 - \mathcal{C}_a^*\mathcal{C}_c) \\ &= t \sum_a \sum_{c\in \mathsf{S}_a} (|\mathcal{C}_c|^2 - \mathcal{C}_c^*\mathcal{C}_a),\end{aligned} \tag{A13}$$

where we have swapped the summations (and relabeled) in the last line making use of Eq. (A7). Now, we can rewrite the matrix element as

$$\begin{aligned}\langle\Psi|H'|\Psi\rangle &= \frac{t}{2} \sum_a \sum_{c\in \mathsf{S}_a} (|\mathcal{C}_a|^2 - \mathcal{C}_a^*\mathcal{C}_c + |\mathcal{C}_c|^2 - \mathcal{C}_c^*\mathcal{C}_a) \\ &= \frac{t}{2} \sum_a \sum_{c\in \mathsf{S}_a} |\mathcal{C}_a - \mathcal{C}_c|^2 \geqslant 0.\end{aligned} \tag{A14}$$

Thus, H' is a positive operator and the flat state $|\Psi_0\rangle$ is the ground state of H at $V = -2t$ for fixed N.

[1] C. H. Bennett and S. J. Wiesner, Communication Via One- and Two-Particle Operators on Einstein-Podolsky-Rosen States, Phys. Rev. Lett. **69**, 2881 (1992).

[2] C. H. Bennett, G. Brassard, C. Crépeau, R. Jozsa, A. Peres, and W. K. Wootters, Teleporting an Unknown Quantum State Via Dual Classical and Einstein-Podolsky-Rosen Channels, Phys. Rev. Lett. **70**, 1895 (1993).

[3] A. K. Ekert, Quantum Cryptography Based on Bell's Theorem, Phys. Rev. Lett. **67**, 661 (1991).

[4] B. Schumacher, Quantum coding, Phys. Rev. A **51**, 2738 (1995).

[5] R. Horodecki, MichałHorodecki, and K. Horodecki, Quantum entanglement, Rev. Mod. Phys. **81**, 865 (2009).

[6] N. Laflorencie, Quantum entanglement in condensed matter systems, Phys. Rep. **646**, 1 (2016).

[7] G. C. Wick, A. S. Wightman, and E. P. Wigner, The intrinsic parity of elementary particles, Phys. Rev. **88**, 101 (1952).

[8] Michał Horodecki, Paweł Horodecki, and R. Horodecki, Limits for Entanglement Measures, Phys. Rev. Lett. **84**, 2014 (2000).

[9] S. D. Bartlett and H. M. Wiseman, Entanglement Constrained by Superselection Rules, Phys. Rev. Lett. **91**, 097903 (2003).

[10] N. Schuch, F. Verstraete, and J. I. Cirac, Nonlocal Resources in the Presence of Superselection Rules, Phys. Rev. Lett. **92**, 087904 (2004).

[11] A. Kitaev, D. Mayers, and J. Preskill, Superselection rules and quantum protocols, Phys. Rev. A **69**, 052326 (2004).

[12] J. Dunningham, A. Rau, and K. Burnett, From Pedigree Cats to Fluffy-Bunnies, Science **307**, 872 (2005).

[13] U. Marzolino and A. Buchleitner, Quantum teleportation with identical particles, Phys. Rev. A **91**, 032316 (2015).

[14] Y. Aharonov and L. Susskind, Charge superselection rule, Phys. Rev. **155**, 1428 (1967).

[15] H. M. Wiseman and J. A. Vaccaro, Entanglement of Indistinguishable Particles Shared between Two Parties, Phys. Rev. Lett. **91**, 097902 (2003).

[16] H. M. Wiseman, S. D. Bartlett, and J. A. Vaccaro, Ferreting out the fluffy bunnies: entanglement constrained by generalized superselection rules, in *Proceedings of the XVI International Conference on Laser Spectroscopy* (World Scientific, Queensland, Australia, 2011), pp. 307–314.

[17] J. A. Vaccaro, F. Anselmi, and H. M. Wiseman, Entanglement of identical particles and reference phase uncertainty, Int. J. Quantum Inf. **01**, 427 (2003).

[18] M. Dowling, A. Doherty, and H. Wiseman, Entanglement of indistinguishable particles in condensed-matter physics, Phys. Rev. A **73**, 052323 (2006).

[19] C. M. Herdman, S. Inglis, P. N. Roy, R. G. Melko, and A. Del Maestro, Path-integral Monte Carlo method for Rényi entanglement entropies, Phys. Rev. E **90**, 013308 (2014).

[20] R. G. Melko, C. M. Herdman, D. Iouchtchenko, P. N. Roy, and A. Del Maestro, Entangling qubit registers via many-body states of ultracold atoms, Phys. Rev. A **93**, 042336 (2016).

[21] I. Klich and L. S. Levitov, Scaling of entanglement entropy and superselection rules, arXiv:0812.0006.

[22] H. Barghathi, C. M. Herdman, and A. Del Maestro, Rényi Generalization of the Accessible Entanglement Entropy, Phys. Rev. Lett. **121**, 150501 (2018).

[23] I. Buluta and F. Nori, Quantum Simulators, Science **326**, 108 (2009).

[24] D. Jaksch and P. Zoller, The cold atom Hubbard toolbox, Ann. Phys. **315**, 52 (2005).

[25] R. Schmied, T. Roscilde, V. Murg, D. Porras, and J. I. Cirac, Quantum phases of trapped ions in an optical lattice, New J. Phys. **10**, 045017 (2008).

[26] T. Byrnes, N. Young Kim, K. Kusudo, and Y. Yamamoto, Quantum simulation of Fermi-Hubbard models in semiconductor quantum-dot arrays, Phys. Rev. B **78**, 075320 (2008).

[27] S. Mostame and R. Schützhold, Quantum Simulator for the Ising Model with Electrons Floating on a Helium Film, Phys. Rev. Lett. **101**, 220501 (2008).

[28] J. Des Cloizeaux, A soluble fermi-gas model. validity of transformations of the bogoliubov type, J. Math. Phys. **7**, 2136 (1966).

[29] Calculations performed using the ITENSOR C++ library (version 2.1.1), http://itensor.org/.

[30] I. Klich, G. Refael, and A. Silva, Measuring entanglement entropies in many-body systems, Phys. Rev. A **74**, 032306 (2006).

[31] P. Calabrese and J. Cardy, Entanglement entropy and quantum field theory, J. Stat. Mech.: Theor. Exp. (2004) P06002.

[32] A. J. Daley, H. Pichler, J. Schachenmayer, and P. Zoller, Measuring Entanglement Growth in Quench Dynamics of Bosons in an Optical Lattice, Phys. Rev. Lett. **109**, 020505 (2012).

[33] M. Goldstein and E. Sela, Symmetry-Resolved Entanglement in Many-Body Systems, Phys. Rev. Lett. **120**, 200602 (2018).

[34] M. B. Hastings, Iván González, A. B. Kallin, and R. G. Melko, Measuring Renyi Entanglement Entropy in Quantum Monte Carlo Simulations, Phys. Rev. Lett. **104**, 157201 (2010).

[35] S. Humeniuk and T. Roscilde, Quantum Monte Carlo calculation of entanglement Rényi entropies for generic quantum systems, Phys. Rev. B **86**, 235116 (2012).

[36] J. McMinis and N. M. Tubman, Renyi entropy of the interacting Fermi liquid, Phys. Rev. B **87**, 081108(R) (2013).

[37] J. E. Drut and W. J. Porter, Hybrid Monte Carlo approach to the entanglement entropy of interacting fermions, Phys. Rev. B **92**, 125126 (2015).

[38] R. Islam, R. Ma, P. M. Preiss, M. Eric Tai, A. Lukin, M. Rispoli, and M. Greiner, Measuring entanglement entropy in a quantum many-body system, Nature (London) **528**, 77 (2015).

[39] A. M. Kaufman, M. Eric Tai, A. Lukin, M. Rispoli, R. Schittko, P. M. Preiss, and M. Greiner, Quantum thermalization through entanglement in an isolated many-body system, Science **353**, 794 (2016).

[40] H. Pichler, G. Zhu, A. Seif, P. Zoller, and M. Hafezi, Measurement Protocol for the Entanglement Spectrum of Cold Atoms, Phys. Rev. X **6**, 041033 (2016).

[41] N. M. Linke, S. Johri, C. Figgatt, K. A. Landsman, A. Y. Matsuura, and C. Monroe, Measuring the Rényi entropy of a two-site Fermi-Hubbard model on a trapped ion quantum computer, Phys. Rev. A **98**, 052334 (2018).

[42] A. Lukin, M. Rispoli, R. Schittko, M. Eric Tai, A. M. Kaufman, S. Choi, V. Khemani, J. Léonard, and M. Greiner, Probing entanglement in a many-body-localized system, Science **364**, 256 (2019).

[43] C. Cachin, Entropy Measures and Unconditional Security in Cryptography, Ph.D. thesis, Swiss Federal Institute of Technology, 1997.

[44] L. Golshani, E. Pasha, and G. Yari, Some properties of rényi entropy and rényi entropy rate, Inf. Sciences **179**, 2426 (2009).

[45] M. Hayashi, Exponential decreasing rate of leaked information in universal random privacy amplification, IEEE T. Inf. Theory **57**, 3989 (2011).

[46] B. Škorić, C. Obi, E. Verbitskiy, and B. Schoenmakers, Sharp lower bounds on the extractable randomness from non-uniform sources, Inf. Comput. **209**, 1184 (2011).

[47] S. Fehr and S. Berens, On the Conditional Rényi Entropy, IEEE T. Inf. Theory **60**, 6801 (2014).

[48] R. Bonsignori, P. Ruggiero, and P. Calabrese, Symmetry resolved entanglement in free fermionic systems, arXiv:1907.02084.

[49] H. Leschke, A. V. Sobolev, and W. Spitzer, Scaling of Rényi Entanglement Entropies of the Free Fermi-Gas Ground State: A Rigorous Proof, Phys. Rev. Lett. **112**, 160403 (2014).

[50] H. F. Song, S. Rachel, and K. Le Hur, General relation between entanglement and fluctuations in one dimension, Phys. Rev. B **82**, 012405 (2010).

[51] H. F. Song, S. Rachel, C. Flindt, I. Klich, N. Laflorencie, and K. Le Hur, Bipartite fluctuations as a probe of many-body entanglement, Phys. Rev. B **85**, 035409 (2012).

[52] P. Calabrese, M. Mintchev, and E. Vicari, Exact relations between particle fluctuations and entanglement in Fermi gases, Europhys. Lett. **98**, 20003 (2012).

[53] C. Holzhey, F. Larsen, and F. Wilczek, Geometric and renormalized entropy in conformal field theory, Nucl. Phys. B **424**, 443 (1994).

[54] P. Calabrese, J. Cardy, and B. Doyon, Entanglement entropy in extended quantum systems, J. Phys. A: Math. Gen. **42**, 500301 (2009).

[55] T. J. Volkoff and C. M. Herdman, Generating accessible entanglement in bosons via pair-correlated tunneling, arXiv:1901.00879.

[56] E. Lieb, T. Schultz, and D. Mattis, Two soluble models of an antiferromagnetic chain, Ann. Phys. **16**, 407 (1961).

[57] J. Des Cloizeaux and M. Gaudin, Anisotropic linear magnetic chain, J. Math. Phys. **7**, 1384 (1966).

[58] F. Franchini, *An Introduction to Integrable Techniques for One-Dimensional Quantum Systems*, Lecture Notes in Physics (Springer, Berlin, 2017).

[59] F. D. M. Haldane, General Relation of Correlation Exponents and Spectral Properties of One-Dimensional Fermi Systems: Application to the Anisotropic S =1/2 Heisenberg Chain, Phys. Rev. Lett. **45**, 1358 (1980).

[60] L. D. Faddeev and L. A. Takhtadzhyan, Spectrum and scattering of excitations in the one-dimensional isotropic heisenberg model, J. Sov. Math. **24**, 241 (1984).

[61] Code, scripts and data for this work are included in a GitHub repository https://github.com/DelMaestroGroup/AccessibleEntanglementFermions.

[62] A. Osterloh, L. Amico, G. Falci, and R. Fazio, Scaling of entanglement close to a quantum phase transition, Nature (London) **416**, 608 (2002).

[63] T. J. Osborne and M. A. Nielsen, Entanglement in a simple quantum phase transition, Phys. Rev. A **66**, 032110 (2002).

[64] S.-Jian Gu, H.-Qing Lin, and Y.-Quan Li, Entanglement, quantum phase transition, and scaling in the XXZ chain, Phys. Rev. A **68**, 042330 (2003).

[65] F. Verstraete, M. A. Martín-Delgado, and J. I. Cirac, Diverging Entanglement Length in Gapped Quantum Spin Systems, Phys. Rev. Lett. **92**, 087201 (2004).

[66] R. Somma, G. Ortiz, H. Barnum, E. Knill, and L. Viola, Nature and measure of entanglement in quantum phase transitions, Phys. Rev. A **70**, 042311 (2004).

[67] A. Anfossi, P. Giorda, A. Montorsi, and F. Traversa, Two-Point Versus Multipartite Entanglement in Quantum Phase Transitions, Phys. Rev. Lett. **95**, 056402 (2005).

[68] D. Larsson and H. Johannesson, Entanglement Scaling in the One-Dimensional Hubbard Model at Criticality, Phys. Rev. Lett. **95**, 196406 (2005).

[69] M. Popp, F. Verstraete, M. A. Martín-Delgado, and J. I. Cirac, Localizable entanglement, Phys. Rev. A **71**, 042306 (2005).

[70] J. Iaconis, S. Inglis, A. B. Kallin, and R. G. Melko, Detecting classical phase transitions with Renyi mutual information, Phys. Rev. B **87**, 195134 (2013).

[71] F. Iemini, T. O. Maciel, and R. O. Vianna, Entanglement of indistinguishable particles as a probe for quantum phase transitions in the extended Hubbard model, Phys. Rev. B **92**, 075423 (2015).

[72] A. Yuste, C. Cartwright, G. De Chiara, and A. Sanpera, Entanglement scaling at first order quantum phase transitions, New J. Phys. **20**, 043006 (2018).

[73] T.-C. Lu and T. Grover, Singularity in entanglement negativity across finite-temperature phase transitions, Phys. Rev. B **99**, 075157 (2019).

[74] C. Walsh, P. Sémon, D. Poulin, G. Sordi, and A.-M. S. Tremblay, Local Entanglement Entropy and Mutual Information across the Mott Transition in the Two-Dimensional Hubbard Model, Phys. Rev. Lett. **122**, 067203 (2019).

[75] D. Braun, G. Adesso, F. Benatti, R. Floreanini, U. Marzolino, M. W. Mitchell, and S. Pirandola, Quantum-enhanced measurements without entanglement, Rev. Mod. Phys. **90**, 035006 (2018).

[76] J. Ren, X. Xu, L. Gu, and J. Li, Quantum information analysis of quantum phase transitions in a one-dimensional $V_1 - V_2$ hard-core-boson model, Phys. Rev. A **86**, 064301 (2012).

[77] Q. Zheng, Y. Yao, and X.-Wei Xu, Probing Berezinskii-Kosterlitz-Thouless Phase Transition of Spin-Half XXZ Chain by Quantum Fisher Information, Commun. Theor. Phys. **63**, 279 (2015).

[78] Y. Chen, P. Zanardi, Z. D. Wang, and F. C. Zhang, Sublattice entanglement and quantum phase transitions in antiferromagnetic spin chains, New J. Phys. **8**, 97 (2006).

[79] Y. Zhang, L. Vidmar, and M. Rigol, Information measures for a local quantum phase transition: Lattice fermions in a one-dimensional harmonic trap, Phys. Rev. A **97**, 023605 (2018).

[80] P. Calabrese, M. Mintchev, and E. Vicari, Entanglement Entropy of One-Dimensional Gases, Phys. Rev. Lett. **107**, 020601 (2011).

[81] P. Calabrese, M. Campostrini, F. Essler, and B. Nienhuis, Parity Effects in the Scaling of Block Entanglement in Gapless Spin Chains, Phys. Rev. Lett. **104**, 095701 (2010).

[82] C. Ning Yang, η-Pairing and Off-Diagonal Long-Range Order in a Hubbard Model, Phys. Rev. Lett. **63**, 2144 (1989).

[83] T. Grover, A. M. Turner, and A. Vishwanath, Entanglement entropy of gapped phases and topological order in three dimensions, Phys. Rev. B **84**, 195120 (2011).

[84] J. R. Garrison, R. V. Mishmash, and M. P. A. Fisher, Partial breakdown of quantum thermalization in a Hubbard-like model, Phys. Rev. B **95**, 054204 (2017).

[85] T. Veness, F. H. L. Essler, and M. P. A. Fisher, Quantum disentangled liquid in the half-filled Hubbard model, Phys. Rev. B **96**, 195153 (2017).

[86] W. S. Bakr, J. I. Gillen, A. Peng, S. Fölling, and M. Greiner, A quantum gas microscope for detecting single atoms in a Hubbard-regime optical lattice, Nature (London) **462**, 74 (2009).

[87] M. Gruber and V. Eisler, Magnetization and entanglement after a geometric quench in the XXZ chain, Phys. Rev. B **99**, 174403 (2019).

[88] H. Barnum, G. Ortiz, R. Somma, and L. Viola, A generalization of entanglement to convex operational theories: Entanglement relative to a subspace of observables, Int. J. Theor. Phys. **44**, 2127 (2005).

[89] K. Schwaiger, D. Sauerwein, M. Cuquet, J. I. de Vicente, and B. Kraus, Operational Multipartite Entanglement Measures, Phys. Rev. Lett. **115**, 150502 (2015).

[90] D. Sauerwein, K. Schwaiger, M. Cuquet, J. I. de Vicente, and B. Kraus, Source and accessible entanglement of few-body systems, Phys. Rev. A **92**, 062340 (2015).

[91] R. Lo Franco and G. Compagno, Indistinguishability of Elementary Systems as a Resource for Quantum Information Processing, Phys. Rev. Lett. **120**, 240403 (2018).

[92] F. Benatti, R. Floreanini, and U. Marzolino, Entanglement in fermion systems and quantum metrology, Phys. Rev. A **89**, 032326 (2014).